

# A Permanent Magnet Free Bearingless Motor For Disposable Centrifugal Blood Pump

Jun Rao<sup>a</sup>, Wataru Hijikata<sup>b</sup> and Tadahiko Shinshi<sup>b</sup>

<sup>a</sup> Department of Mechano-Micro Engineering, Tokyo Institute of Technology, Yokohama, Japan, shinshi@pi.titech.ac.jp

<sup>b</sup> Precision and Intelligence Laboratory, Tokyo Institute of Technology, Yokohama, Japan

**Abstract**—The disadvantages of disposable centrifugal blood pumps (DCBPs) are the high cost of the disposable pump head due to the use of rare earth magnets and the complex-shaped secondary flow channel due to the space allocated for the magnetic coupling. In order to overcome these problems a permanent magnet free bearingless motor for DCBPs with a smooth secondary flow channel has been developed. The radial position and rotational speed of the rotor are actively controlled, and the axial position and tilt angle of the rotor are passively stabilized by a magnetic reluctance force. Results of magnetic field FEM analysis showed that the proposed bearingless motor has an axial stiffness of 3.50 N/mm and a tilt stiffness of 0.87 Nm/rad. In an experiment, the power consumption of the prototype was less than 30 W without load at a rotational speed of 3000 rpm.

## I. INTRODUCTION

To support blood circulation in heart failure patients, various types of blood pump have been developed and used at the clinical stage. In recent years, rotary blood pumps such as centrifugal and axial pumps, which generate continuous flow by rotating an impeller, have made progress in research and practical use [1].

Up till now, disposable centrifugal blood pumps (DCBPs) whose single-use pump heads can easily be attached to and detached from a reusable unit, have been used for circulation support in cardiopulmonary bypass operations, for extracorporeal membrane oxygenation, and for emergency circulatory resuscitation [2][3]. Not only the pressure-flow characteristics, but also prolonged durability, minimal destruction of blood cells (hemolysis), and no thrombus formation are important requirements for DCBPs. Furthermore, cost-effective disposable pump heads are also required for DCBPs.

Contactless support of the impeller by a magnetic bearing has been identified as a promising method for reducing blood damage and enhancing durability [4]-[7]. Our group has developed a DCBP employing a two-degree-of-freedom magnetic bearing [4]. Nevertheless, the shape of the secondary flow channel is very complicated due to the space allocated for the magnetic bearing and the contactless torque transmission mechanism as shown in Fig. 1. The complex secondary channel leads to small tolerances in manufacturing and a difficult fabrication process. A DCBP utilizing bearingless motor technology has also been proposed [5]. The disposable pump head of this DCBP utilizes a rare earth magnet. However, rare earth magnets increase the cost of the

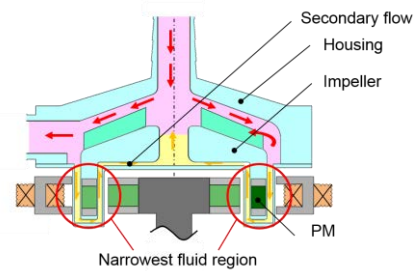


Figure 1 Disposable pump head structure of a previously proposed DCBP

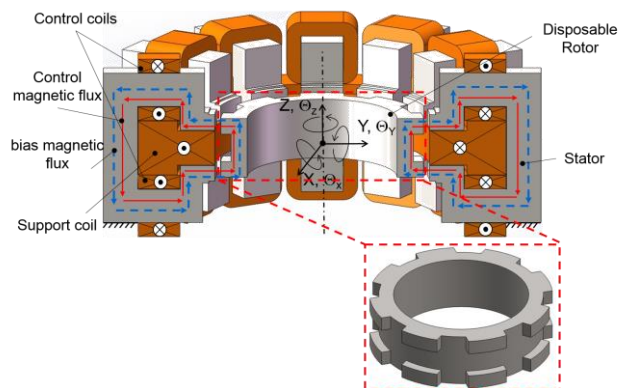


Figure 2 Structure of proposed bearingless motor

disposable pump head as well as causing serious damage to the environment during the mining and fabrication processes of the rare earth elements.

In this paper, a prototype bearingless motor for potential application in a DCBP is proposed. The proposed bearingless motor has a permanent magnet free rotor and a permanent magnet free magnetic bearing structure which is arranged around the rotor. Thus, a cost-effective pump head with a simple-shaped secondary flow channel can be achieved.

## II. BEARINGLESS MOTOR FOR DCBP

### A. Structure

Figure 2 shows the configuration of the proposed bearingless motor which is a hybrid of a two-degree-of-freedom controlled magnetic bearing and a three-phase twelve-eight-pole switched reluctance motor. The stator core consists of twelve C-shaped cores made of soft magnetic material allocated around the rotor at even intervals. Each core has a pair of square-shaped control coils placed symmetrically

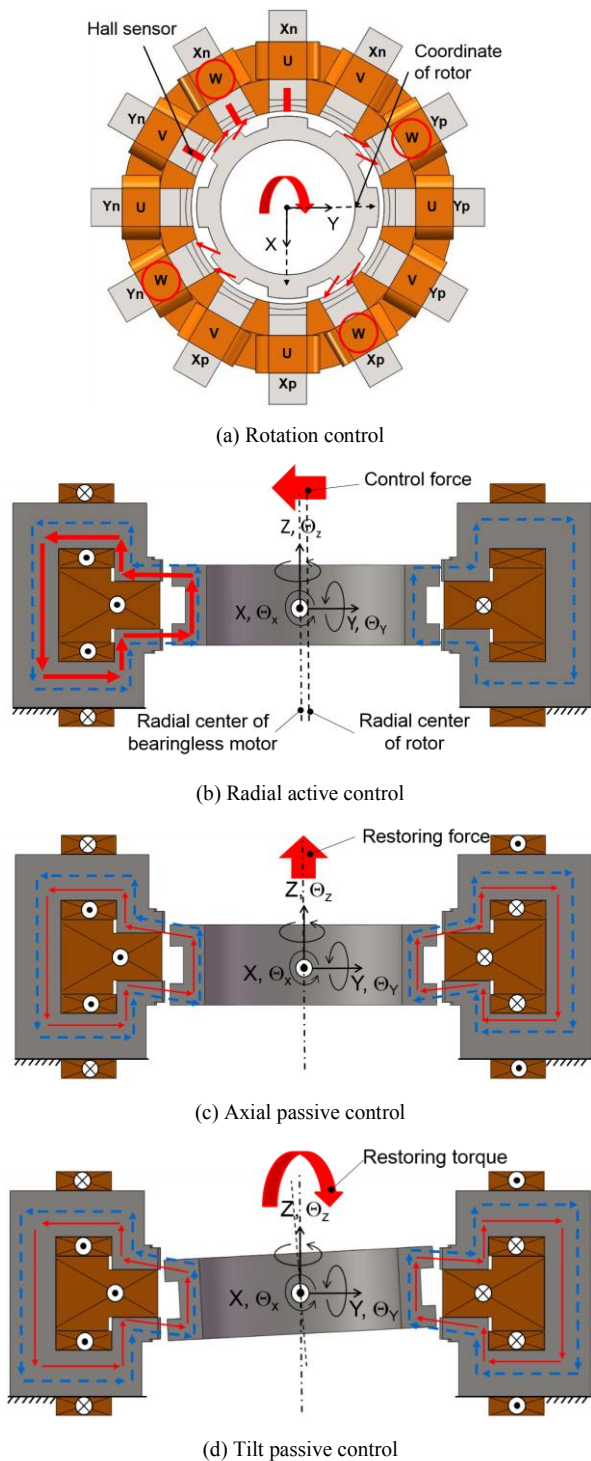


Figure 3 Control principle of proposed bearingless motor

in the axial direction. To rotate the rotor, a control magnetic flux is generated between the C-shaped stator cores and the rotor by applying current to the control coils. There is a large ring-shaped support coil wound in the stator core concentric with the rotor so that a bias magnetic flux is generated between the C-shaped stator cores and the rotor when a constant current is applied. This unique structure makes the

proposed bearingless motor permanent magnet free and compact.

### B. Rotation

The twelve stator cores are divided into four groups ( $X_p$ ,  $X_n$ ,  $Y_p$  and  $Y_n$ ) for radial positioning control and three phase groups (U, V and W) for rotational control as shown in Fig. 3(a). Thus, during rotation of the rotor, the control current in each control coil is the sum of the positioning current and the rotational current. When the rotational angle of the rotor is at the position shown in Fig. 3(a), rotational current is applied to the four pairs of control coils in the W phase group to generate a rotational torque in the clockwise direction. The three Hall element sensors are used to measure the phase and its rate of change and calculate the rotational speed of the rotor. Thus, the proposed bearingless motor works as a traditional three-phase twelve-eight-pole switched reluctance motor.

### C. Radial Suspension Force Generation

Figure 3(b) shows the magnetic circuit and the principle by which the positioning force is generated in the radial direction. The solid red and dashed blue lines indicate the control and bias magnetic fluxes, respectively. When the rotor leaves the radial center of the motor as shown in Fig. 3(b), for example, the displacement sensor will detect the error. The positioning current in the square-shaped coils wound on the C-shaped stator cores which are located in the same direction as the rotor displacement (positive Y direction, as shown in Fig. 3(b);  $Y_p$  stator group, as shown in Fig. 3(a)) will be zero. There will be positioning current in the square-shaped coils only on the opposite side (negative Y direction, as shown in Fig. 3(b);  $Y_n$  stator group, as shown in Fig. 3(a)). This current difference will generate a force in the Y direction. As a result, the rotor will be drawn back and kept in the radial center of the bearingless motor. This positioning method is different from the conventional one [8]. In the conventional positioning method, a bias magnetic flux on the same side as the rotor displacement is weakened by supplying a “reverse positioning current” to the control coil, which leads to lower control efficiency. Additionally, this reverse positioning current will weaken the axial and tilt stiffness of the rotor. On the other hand, in the proposed method no current is used to substitute for this reverse positioning current.

### D. Passive Stabilization

Figures 3(c) and (d) show schematics of the passive stabilization of the rotor in the axial and tilt directions. The axial and tilt motions of the rotor are passively stabilized by a reluctance force generated from the bias and control magnetic fluxes. The axial and tilt stiffnesses are enhanced during rotation of the rotor because of the rise in control current leading to an increase in the control magnetic flux. Thus, due to the increase in stiffness, the rotor can be levitated more stably.

### E. Bearingless Motor Prototype

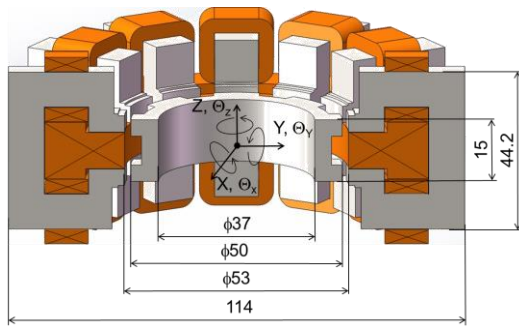


Figure 4 Design of the proposed bearingless motor

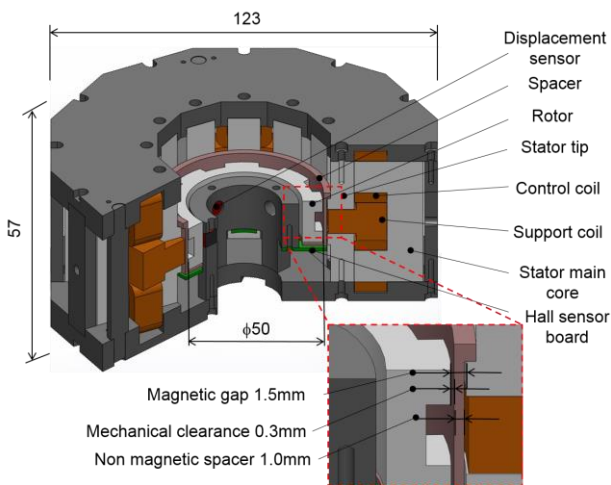


Figure 5 Mechanical structure

DCBPs are required to yield a flow rate of 5 L/min against a head pressure of more than 250 mmHg (33.3 kPa) for extracorporeal circulation support with the use of an artificial lung. According to our previously proposed magnetically-levitated DCBP with a 50 mm diameter impeller [8], a rotational speed of over 3000 rpm is necessary. Following the design aspects of our previous research, we employed a rotor with a diameter of 50 mm with a target rotational speed of 3000 rpm.

Figure 4 shows the dimensions of the proposed bearingless motor. The origin of the system is at the geometric center of the rotor. The height of the rotor is 15 mm. As shown in Fig. 5, the total height and diameter of the proposed motor is 57 mm and 123 mm, respectively. The mass of the rotor is 0.074 kg which was directly measured on precision scales. The magnetic gap between the rotor, which is made of soft iron, and the stator cores is 1.5 mm. Additionally, for future DCBPs, the mechanical clearance between the rotor and the housing wall of the pump head is 0.3 mm which is large enough to avoid substantial destruction of blood cells (hemolysis). A spacer with a thickness of 1.0 mm is placed between the stator and the rotor to generate a mechanical clearance of 0.3 mm in the prototype. In order to decrease the eddy current loss, laminated steel with a lamination thickness of 0.35 mm is used to fabricate parts of the C-shaped stator core. Due to the two-dimensional slice structure of laminated steel and the complex three-dimensional geometry of the C-shaped stator cores, each

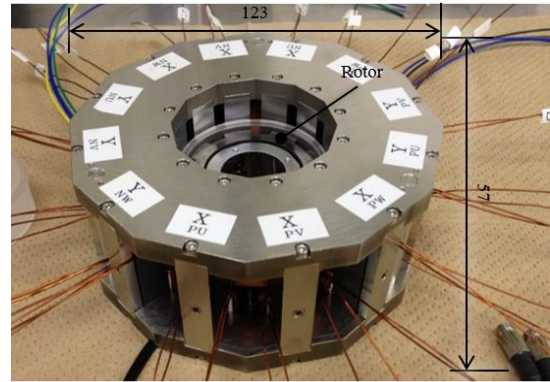


Figure 6 Fabricated bearingless motor

C-shaped stator core is divided into three parts. The main part of the stator core is made of laminated steel and the two tip cores are made of soft iron. An overview of the prototype is shown in Fig. 6. The control and support coils have 75 and 196 turns, respectively. The diameters of the wires in the control and support coils are 0.6 mm and 0.95 mm, respectively. For convenience, the three eddy current displacement sensors (PU-05A, AEC Corp., Japan) are allocated on the inner side of the rotor in this prototype design. For future DCBPs, the displacement sensors will be put on the outer side of the rotor.

## III. SIMULATION AND EXPERIMENT

### A. Stiffness Simulation

In order to achieve continuous work, the maximum thermal balance temperature of the support coil is set to 65°C. During thermal testing of the support coil, a bias current of 3.6A achieved a thermal balance temperature of less than 65°C after over half an hour of continuous work at room temperature of 25°C. Figure 7 shows the simulation performance of the proposed bearingless motor under stop mode (0 rpm) and rotation mode with a phase current of 1A. The bias current in the support coil is set to 3.6A in order to generate a stable and sufficient bias magnetic flux between the rotor and the stator and to achieve continuous work. Both the axial stiffness and the tilt stiffness increase by 15% and 13%, respectively, during rotation of the motor, because the rise in control current leads to a rise in the control magnetic flux. This enhancement in stiffness during rotation provides the possibility of us being able to reduce the bias current in future research.

### B. Motor Performance Measurement

The rotational accuracy and power consumption of the prototype were evaluated experimentally. Large vibration amplitudes of the impeller and heat generated by the coils cause hemolysis. In order to stabilize the magnetic levitation and reduce heat generation, a pole-placement controller and a zero-power controller [9], respectively, were adopted for the control system. The viability of the zero-power controller was evaluated under conditions in which the rotor rotates without a load at room temperature (25°C).

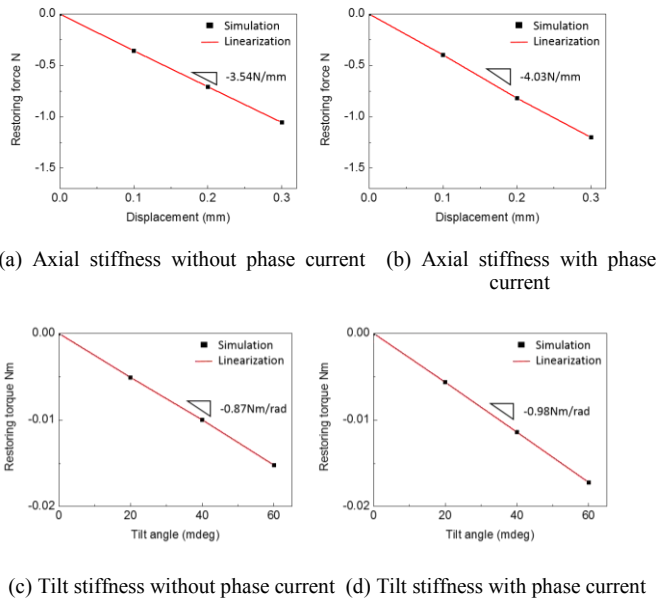


Figure 7 Stiffness simulation results of the proposed bearingless motor

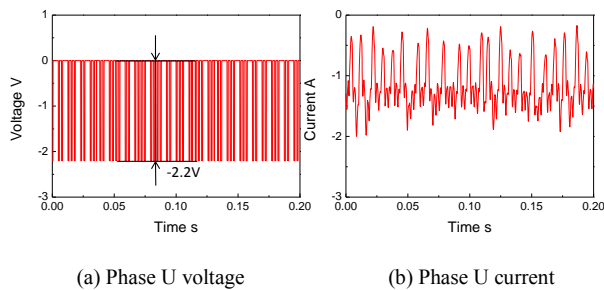


Figure 8 Phase U voltage and current at 3,000rpm

In measurements of the performance, the motor was rotated without load under a bias current of 3.6 A which flows through the support coil. The power consumption of the motor was calculated using the feedback signal provided by the current sensor. During the measurement, the rotational speed of the rotor was under closed-loop control. The measured vibration amplitude of the rotor in the X direction at 3000 rpm without a load was less than  $\pm 25\mu\text{m}$ , which is sufficiently smaller than the mechanical clearance of 0.3 mm.

Figures 8 (a) and (b) show the phase U voltage and current of the fabricated motor at a target speed of 3000 rpm. The power consumption of one pair of control coils is 0.68 W at a rotational speed of 3000 rpm, and the power consumption of the support coil with a resistance of  $1.66\ \Omega$  is 21.5 W at a bias current of 3.6 A. The total power consumption of the motor is 29.7 W. Over 70% of the power is consumed by the support coil. Thus, the power consumption of the support coil needs to be reduced.

Adjusting the bias current based on the control current is a solution for reducing the total power consumption without decreasing the passive stiffness.

Figures 9 (a) and (b) show the maximum rotational speed and phase U current of the motor. The maximum speed is over 3200 rpm. The average phase U current has increased

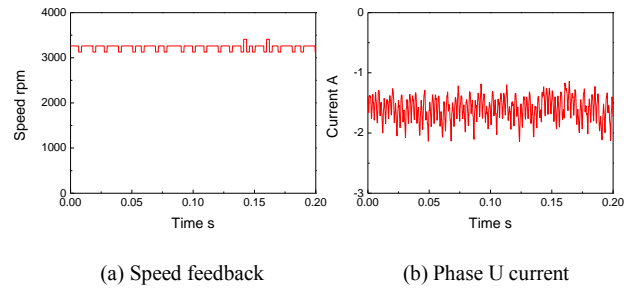


Figure 9 Maximum speed test

significantly compared with that shown in Figure 8 (b). This is because of the magnetic saturation of the stator and the eddy current generated during the high speed phase transformation.

#### IV. CONCLUSIONS

A bearingless motor for a DCBP with a permanent magnet free structure was designed and fabricated. The positioning and rotational performance of the motor was evaluated. The rotor can be levitated and rotated at a maximum speed of over 3200 rpm with a rotational error of less than  $\pm 25\ \mu\text{m}$ . The power consumption of the proposed motor is less than 30 W at a rotational speed of 3000 rpm.

Future work is to reduce the bias current in the support coil and fabricate a DCBP using this proposed bearingless motor.

#### ACKNOWLEDGEMENT

This research is partly supported by JSPS KAKENHI Grant Number 24360059.

#### REFERENCES

- [1] Takatani S, "Progress of rotary blood pumps," *Artificial Organs*, vol. 30, no.5, pp.317-321, 2006.
- [2] George PN, Javier AL, and Suellen I. "Acute and temporary ventricular support with bioMedicus centrifugal pump." *Ann Thorac Surg* vol. 68, pp. 650-4, 1999.
- [3] U.Mehlhorn, et al, "LIFEBRIDGE: a portable, modular, rapidly available "plug-and-play" mechanical circulatory support system." *Ann Thorac Surg*, Vol. 80, no. 5, pp. 1887-1892, 2005
- [4] Hijikata W, Shinshi T, Asama J, et al. A magnetically levitated centrifugal blood pump with a simple-structured disposable pump head. *Artificial Organs* 2008;32:531-40.
- [5] Schob R, Barletta N. Principle and application of a bearingless slice motor. *JSME Int J Ser C* 1997;40:593-8.
- [6] Someya T, Kobayashi M, Waguri S, et al. Development of a disposable Mag-lev centrifugal blood pump(MedTech Dispo) intended for one-month support in bridge-to-bridge applications: in vitro and initial in vivo evaluation. *Artificial Organs* 2009;33:704-13.
- [7] Hijikata W, Mamiya T, Shinshi T, Takatani S. A cost-effective extracorporeal magnetically-levitated centrifugal blood pump employing a disposable magnet-free impeller. *Proc. IMechE, J.Engineering in Medicine*, Vol.225, pp.1149-1157, Dec. 2011.
- [8] Hijikata W, Sobajima H, Shinshi T, et al, "Disposable MagLev centrifugal blood pump utilizing a cone-shaped impeller." *Artificial Organs* 2010, vol. 34, pp. 669-677.
- [9] Mizuno T, Takasaki M, Suzuki H, Ishino Y, "Development of a three-axis active vibration isolation system using zero-power magnetic suspension." *Proceedings of the 42<sup>nd</sup> IEEE Conference on Decision and Control*, pp. 4493-4498, 2003.